



HHS Public Access

Author manuscript

Nat Genet. Author manuscript; available in PMC 2012 April 01.

Published in final edited form as:

Nat Genet. ; 43(10): 1026–1030. doi:10.1038/ng.915.

Germline deletion of the miR-17-92 cluster causes growth and skeletal defects in humans

Loïc de Pontual^{1,2,10}, Evelyn Yao^{3,10}, Patrick Callier⁴, Laurence Faivre⁴, Valérie Drouin⁵, Sandra Cariou¹, Arie Van Haeringen⁶, David Geneviève⁷, Alice Goldenberg⁵, Myriam Oufadem¹, Sylvie Manouvrier⁸, Arnold Munnich^{1,9}, Joana Alves Vidigal³, Michel Vekemans¹, Stanislas Lyonnet^{1,9}, Alexandra Henrion-Caude¹, Andrea Ventura^{3,10}, and Jeanne Amiel^{1,9,10}

¹Unité INSERM U-781, Université Paris Descartes, Paris, France ²Services de Pédiatrie, Hôpital Jean Verdier, Université Paris XIII, AP-HP, Bondy, France ³Cancer Biology and Genetics Program, Memorial Sloan-Kettering Cancer Center, New York, New York 10065, USA ⁴Service de Génétique, Hôpital d'enfants, Dijon, France ⁵Service de Génétique, Hôpital Charles Nicolle, Rouen, France ⁶Department of Human and Clinical Genetics, Leiden University Medical Center, Leiden, The Netherlands ⁷Service de Génétique, Hôpital Arnaud de Villeneuve, Montpellier, France ⁸Service de Génétique Clinique, Hôpital J. de Flandre, Lille, France ⁹Services de Génétique et cytogénétique, Hôpital Necker-Enfant Malades, AP-HP, Paris, France

Introduction

MicroRNAs (miRNAs) have emerged as key regulators of gene expression in animal and plants. Studies in a variety of model organisms have provided overwhelming evidence that miRNAs modulate developmental processes. Nevertheless, the only hereditary condition known to be caused by a miRNA is a form of adult-onset non-syndromic deafness¹, and no

Users may view, print, copy, download and text and data- mine the content in such documents, for the purposes of academic research, subject always to the full Conditions of use: http://www.nature.com/authors/editorial_policies/license.html#terms

Correspondence should be addressed to: Jeanne Amiel, Département de Génétique, Hôpital Necker-Enfants Malades, 149, rue de Sèvres, 75743 Paris Cedex 15, France. Phone: 33 1 44495648, Fax: 33 1 44495150, Jeanne.amiel@inserm.fr and Andrea Ventura, Cancer Biology and Genetics Program, Memorial Sloan-Kettering Cancer Center, 1275 York Avenue, New York, NY, 10065, Phone: +1-646-888-3068, Fax: 646-422-0871, venturaa@mskcc.org.

¹⁰These authors contributed equally to this work

Authors Contributions

L.P., P.C., S.C., and M.O. performed patient-related experiments. E.Y. performed the analysis of miR-17-92 mutant mice, the ChIP experiments, and determined miR-17-92 expression in patients. J.A.V. determined miR-17-92 expression in mouse embryos. J.A. and A.V. designed and supervised the project and wrote the manuscript. A.M., M.V., S.L., L.P., E.Y., and A.H-C provided critical input into project development and manuscript preparation. All other coauthors identified subjects with FS and performed related clinical and laboratory studies (L.F., V.D., A.V.H., D.G., A.G., S.M.).

COMPETING FINANCIAL INTERESTS

The authors declare no competing financial interests.

URLs

OMIM: <http://www.ncbi.nlm.nih.gov/omim/>

Ensembl: www.ensembl.org

Database of Genomic Variants: <http://projects.tcag.ca/variation/>

1000 Genomes Browser: <http://browser.1000genomes.org/index.html>

UCSC Genome Assembly: <http://genome.ucsc.edu/>

miRNA mutation has yet been found to be responsible for a developmental defect in humans.

Here we report the identification of germline hemizygous deletions of *MIR17HG*, encoding the miR-17~92 polycistronic miRNA cluster, in patients with microcephaly, short stature and digital abnormalities. We demonstrate that haploinsufficiency of miR-17~92 is responsible for these developmental abnormalities by showing that mice harboring targeted deletion of the miR-17~92 cluster phenocopy several key features of the patients.

These findings uncover a novel regulatory function for miR-17~92 in growth and skeletal development and represent the first example of a miRNA gene responsible for a syndromic developmental defect in humans.

Results and Discussion

The *MIR17HG* locus encodes for miR-17~92, a polycistronic miRNA cluster from which six distinct miRNAs are produced (Supplementary Fig. 1). Genetic and functional studies have provided overwhelming evidence that this cluster is a *bona fide* human oncogene^{2–10}. In addition, loss of function experiments in mice have shown that miR-17~92 is essential for mammalian development and that its complete inactivation leads to perinatal lethality¹¹.

Feingold syndrome (FS, MIM164280) is an autosomal dominant syndrome whose core features are microcephaly, relative short stature and digital anomalies, particularly brachymesophalangy of the second and fifth fingers and brachysyndactyly of the toes^{12,13}. Less penetrant defects include oesophageal/duodenal atresia (observed 30–55% of cases), heart and kidney defects and variable learning disabilities. In approximately 70% of affected families, FS is caused by germline loss-of-function mutations of the *MYCN* gene (MIM 164840) at 2p24.1^{14,15}, but the genetic lesion(s) responsible for the remaining cases have yet to be identified.

We employed high-resolution comparative genomic hybridization (CGH) arrays to perform a genome-wide analysis of 10 index patients displaying skeletal abnormalities consistent with a diagnosis of FS, but lacking any mutation at the *MYCN* locus (Supplementary Table 1). This led to the identification of germline hemizygous microdeletions at 13q31.3 in two cases (AO39 II3 and AO70 II1, Fig. 1 and Fig. 2A). The deletion in AO39 II3 spans 2.98 Mb and encompasses three genes: *LOC144776*, *MIR17HG*, and *Glypican-5* (*GPC5*). The deletion identified in AO70 II1 is more informative as it spans 165 kb and encompasses only miR-17~92 and the first exon of *GPC5* (Fig. 2A). qPCR and direct sequencing of *MIR17HG* (including the promoter region) and of the *GPC5* coding sequence failed to identify non-annotated sequence variations in the remaining eight index cases (data not shown, the primers used are listed in Supp. Table 2).

By genomic qPCR, we determined that the deletions detected in the two index cases segregate with the disease in the two families (Fig. 2B), thus lending support to the hypothesis that these two microdeletions are the causative mutations in these patients.

Next, we queried the DECIPHER database, which contains array CGH data from more than 6000 individuals with a variety of disorders¹⁶ and identified an additional individual (patient id: 248412) harboring a 180kb hemizygous 13q31.3 microdeletion encompassing the entire *MIR17HG* locus and the first exon of *GPC5* (Fig. 1 and 2A). This deletion was further confirmed by genomic qPCR (Figure 2B). Unfortunately, due to the lack of any genetic and clinical data from the parents of this individual, it is unclear whether the deletion was inherited or *de novo*. Although not classified as having FS, the patient presents a combination of features compatible with a diagnosis of FS (Fig. 1 and Supplementary Table 1). The only exception was the presence of unusually hypoplastic thumbs, a trait we also observed in patient A070P (Fig. 1 and Supplementary Table 1) and one that is rarely as severe in *MYCN*-mutant FS patients¹⁵. Analogous digital abnormalities were previously reported in some individuals presenting large 13q deletions^{17,18}; however, due to the large size of the deletions, the gene(s) responsible for the developmental defects could not be identified.

To determine whether hemizygous loss of *MIR17HG* in humans results in a detectable reduction of miR-17~92 expression, we performed RT-qPCR on total RNA extracted from white blood cells obtained from three individuals carrying the 13q31.3 microdeletions. In these patients, expression of all six microRNAs encoded by the miR-17~92 cluster was approximately 50% relative to control individuals (Fig. 2C). This indicates that hemizygous loss of miR-17~92 results in a significant reduction in the expression of its constituent miRNAs that is not compensated by up-regulation of the remaining allele.

Together, these findings suggest that hemizygous deletion of *MIR17HG* and/or *GPC5* is responsible for the skeletal abnormalities observed in these patients, but do not define the relative contribution of either gene. To address this issue, we first queried the Database of Genomic Variants (DGV)¹⁹, which compiles structural variations detected in the genomes of healthy individuals (<http://projects.tcag.ca/variation/?source=hg19>). We identified two Yoruba control individuals²⁰ heterozygous for a deletion encompassing exon 4 of *GPC5* (Supplementary Fig. 2), which is predicted to produce a loss-of-function allele, as exon 3 and exon 5 are not in frame. Moreover, the 1000 genomes browser (<http://browser.1000genomes.org/index.html>) reports a single nucleotide insertion in the coding sequence of *GPC5* (rs34433071, c.1356_1357insC, p. Val454CysfsX7). Although the allelic frequency of this variant is currently unknown, the insertion is predicted to result in the loss of the 113 C-terminal amino acids of *GPC5*. In contrast, although a ~1.8 kbp deletion ending 1.4 kbp upstream of the first miRNA of the miR-17~92 cluster is reported in five normal individuals (Supplementary Fig. 2), no structural variants or polymorphisms directly affecting the miRNAs encoded by the cluster were identified in these databases. Collectively, these data indicate that hemizygous loss of *GPC5* alone cannot account for the phenotypes observed in our patients. To determine whether this can be explained by miR-17~92 haploinsufficiency, we next examined the consequences of hemizygous deletion of this cluster in mice¹¹.

Animals harboring targeted deletions of a single miR-17~92 allele (miR-17~92^{+/−}) are viable and fertile but significantly smaller than wild type controls¹¹ (Fig. 3A), a feature also observed in both *MYCN*-mutant FS patients and patients harboring 13q31.3 microdeletions. Skeletal analysis of the limbs from age- and sex-matched wild-type and miR-17~92^{+/−} adult

mice revealed a striking shortening of the mesophalanx of the fifth finger in heterozygous animals (Figs. 3B and C), another feature observed in patients with 13q31.3 microdeletions and in virtually all FS patients¹⁵. Other long bones in the hands of miR-17~92^{+/+} mice were only marginally shorter (Fig. 3B and data not shown) and syndactyly was not observed in any of the hemizygous animals. Analysis of the skull revealed shortening of the anterior-posterior axis and an overall reduction in size, which are both consistent with microcephaly (Fig. 3D). Importantly, though *Gpc5* and miR-17~92 are also closely linked in the mouse genome, targeted deletion of miR-17~92 does not negatively affect the expression of *Gpc5* in the forelimbs of developing mouse embryos or in mouse embryo fibroblasts (Supplementary Fig. 3 and data not shown), further demonstrating that miR-17~92, but not *Gpc5* is responsible for the key features observed in miR-17~92^{+/+} mice and patients harboring del13q31.3.

Prompted by these findings, we examined the consequences of complete loss of miR-17~92 function on skeletal development. Because homozygous deletion of the cluster leads to perinatal lethality in mice¹¹, we analyzed animals at embryonic day 18.5 (E18.5). Skeletal preparations of miR-17~92^{-/-} embryos revealed a severe and general delay of endochondral and membranous ossification (Fig. 4). Strikingly, the main limb defects observed in FS patients were grossly exacerbated in these animals. More specifically, we observed the complete absence of the mesophalanx of the fifth digit, the presence of a small mesophalanx of the second digit, and hypoplasia of the first digital ray (Fig. 4A and Supplementary Fig. 4). In addition, all embryos examined presented with fusion of cervical vertebrae (Fig. 4B and Supplementary Fig. 4) and microcephaly (Figs. 4C and D). Additional skeletal defects consistently observed in these embryos included dysmorphic zeugopods and fusion of the proximal carpal bones (Fig. 4A and Supplementary Fig. 4). In sum, the human genetic data and the analysis of miR-17~92^{-/-} and miR-17~92^{+/+} mice demonstrate that miR-17~92 haploinsufficiency is responsible for developmental abnormalities in humans and highlight a previously unappreciated role for miR-17~92 in normal growth and skeletal development.

Based on the similarities between the skeletal defects observed in FS patients harboring *MYCN* mutations and in patients with hemizygous deletion of *MIR17HG*, it is tempting to speculate that these two genes may be components of the same developmental pathways and that miR-17~92 may be an important target of *MYCN* in skeletal development. Indeed, several lines of evidence indicate a close genetic and functional interaction between the *MYC* family of transcription factors (*MYC*, *MYCN* and *MYCL*) and the miR-17~92 cluster. Both *MYC* and *MYCN* can activate the transcription of miR-17~92 (refs. ^{2,6,21-24}, Supplementary Figure 5 and Supplementary Note) and can directly bind to the miR-17~92 promoter region in human and murine cells (refs. ^{21,24,25} and Supplementary Fig. 6). Furthermore, ectopic expression of miR-17~92 cooperates with *Myc* in murine models of B-cell lymphoma and colorectal cancer^{4,5,26}. A possible cooperation between *MYCN* and miR-17~92 in modulating developmental processes is further supported by the remarkable similarity of the phenotypes observed in miR-17~92^{-/-} mice and in mice carrying hypomorphic or null *Mycn* alleles (Supplementary Table 3)²⁷⁻²⁹.

One hypothesis emerging from these observations is that *MYCN* regulates various aspects of mammalian development via transactivation of miR-17~92. This hypothesis can be

further refined by considering the phenotypic differences between mice carrying mutant alleles of *Mycn* and miR-17~92 and by comparing the consequences of *MYCN* and miR-17~92 loss in patients. For example, while FS patients with *MYCN* haploinsufficiency frequently present with gastrointestinal atresia (55% of cases)¹⁵, this phenotype was not observed in any of the six miR-17~92 mutant patients described here, nor was it observed in miR-17~92^{+/+} or miR-17~92^{-/-} mice (data not shown). Because abnormal gut development is reported in *Mycn*^{-/-} mice (refs. ^{30,31} and Supplementary Table 3), it seems plausible that *MYCN* controls gastrointestinal development independently of miR-17~92, or that miR-17~92 is functionally redundant. In contrast, microcephaly, short stature and brachymesophalangy are seen in *MYCN*- and miR-17~92-mutant patients and mice, indicating functional cooperation between these two genes in skeletal development and growth.

Because none of the individuals with a *MIR17HG* deletion have gastrointestinal atresia, whether they should be classified as true FS cases or as affected by a novel form of brachydactyly with short stature and microcephaly remains an open question. Nevertheless, our results provide a strong rationale for testing all patients displaying skeletal features of FS for mutations in both *MYCN* and *MIR17HG*.

At present, the detailed molecular mechanisms and the targets through which miR-17~92 modulates skeletal development remain unknown and will be the subject of future studies. Yet, it is worth noting that miR-17~92 has been shown to modulate the TGF-beta and Sonic Hedgehog axes^{6,10,32-34}, two of the most important signaling pathways controlling skeletal development and limb patterning.

Although our analysis of miR-17~92^{+/+} mice clearly indicates that reduced dosage of this cluster can generate many of the skeletal phenotypes observed in FS patients with *MYCN* mutation and in patients harboring 13q31.3 microdeletions, we cannot exclude the possibility that *GPC5* haploinsufficiency also contributes to the pathogenesis of some of these phenotypes. In particular, it is possible that *GPC5* haploinsufficiency plays a role in the severe thumb hypoplasia observed in some individuals carrying 13q31.3 microdeletions. Addressing this issue will require the identification and characterization of additional families carrying deletions of this region and the generation of miR-17~92 and *Gpc5* compound-mutant animals.

In conclusion, this study provides the first evidence of a germline mutation of a miRNA gene leading to a developmental defect in humans. Together with the previous report of mutation of miR-96 in adult onset hereditary deafness¹, miR-17~92 represents the only other known example of a miRNA directly responsible for a hereditary disease in humans. Our results also expands the known biological activities of a major oncogenic miRNA cluster by demonstrating its role in skeletal growth and patterning, and suggests a possible functional interaction between *MYCN* and miR-17~92 in modulating embryonic development.

Material and Methods

Patients

Patients were referred by their clinical geneticists as possible Feingold syndrome cases for molecular analysis. Informed consent was obtained from all subjects or from their legal tutor. Clinical diagnostic criteria included three or more of the core features for FS, namely: i) microcephaly, ii) brachymesophalangy, iii) facial features compatible with those previously described in Feingold patients and iv) oesophageal or duodenal atresia. Patients included in the series had no mutation in the *MYCN* coding sequence and no deletion encompassing the locus³⁵. The clinical data for each patient are summarized in Supplementary Table 1.

Array comparative genomic hybridization (CGH)

Array-CGH was performed using the Agilent Human Genome CGH Microarray Kit 105K and 244K (Agilent Technologies, Santa Clara, CA)³⁶. Array-CGH analysis was performed according to the Agilent protocol with minor protocol modifications: DNA was labeled by direct incorporation of Cya-5 and Cya-3 using an Oligo-array kit (Enzo) for 4 hr and purified by QIAmp DNA Mini kit (Qiagen, Valencia, CA). A graphical overview was obtained using Genomic Workbench software (v5.0), and the statistical algorithm ADM-2, according to a sensitivity threshold of 6.0 and a moving average window of 0.5 Mb. Mapping data were analyzed on the human genome sequence using Ensembl (www.ensembl.org). Copy Number Variations were assessed in the Database of Genomic Variants (<http://projects.tcag.ca/variation/>). An Affymetrix 500k was used for the patient quoted in DECIPHER.

Quantitative real-time PCR (qPCR)

Blood samples were obtained with informed consent for molecular analysis and DNA was extracted according to standard protocols. Primers were designed to amplify the pri-miR-17~92 region chosen, and *MYCN* was used as a reference gene (sequences of primers are listed in Supplementary Table 3). Micro-rearrangements in the DECIPHER case, AO39 II3 and AO70 II1 were tested in all available members of the two families by semi-quantitative PCR on a Mastercycler® Realplex machine (Eppendorf) using the GoTaq® qPCR Master Mix protocol.

Total RNA from peripheral white blood cells of patients and healthy controls was extracted using a standard Trizol protocol. Expression of the miR-17~92 cluster of miRNAs was determined with Taqman miRNA expression assays (Applied Biosystems) according to the manufacturer's instructions. Samples were assayed in quadruplicate and normalized to sno135.

Mouse Husbandry

All animal studies and procedures were approved by the MSKCC Institutional Animal Care and Use Committee. Mice were maintained in a mixed 129SvJae and C57/B6 background. miR-17~92^{+/+} and miR-17~92^{-/-} mice have been previously described¹¹.

Skeletal Preparations

E18.5 embryos were eviscerated and soaked in ddH₂O for 3 hours at room temperature. Fetuses were heat-shocked in a 65°C water bath for 1 minute to facilitate skinning. Adult mice were sacrificed by CO₂ asphyxiation, skinned and eviscerated. All carcasses were fixed in 100% EtOH and incubated in alcian blue (150mg/L alcian blue 8GX, 80% ethanol, 20% acetic acid) and alizarin red (50mg/L alizarin red S in 2% KOH) to stain for cartilage and bone, respectively. Remaining tissues were cleared in 2% KOH-ddH₂O and skeletons were placed in 25% glycerol-ddH₂O for storage. Images were captured with a Zeiss Stereo Discovery V8 microscope and processed in Photoshop. Images were acquired at the same magnification to allow for direct comparison between different genotypes.

Measurements of digit length were performed in Image J and ratios were determined by measuring the length of the 5th mesophalanx from each limb and normalizing to the 5th metacarpal.

pri-miR-17~92 and *GPC5* direct sequencing

The PCR reaction mixture (25 µl) contained 100 ng of leukocyte DNA, 20 pmol of each primer (Supplementary Table 3), 0.1 µM dNTP and 1 U *Taq* DNA polymerase [Invitrogen]. DNA sequencing of the coding exons and intronic flanking regions was performed by the fluorometric method on both strands [ABI BigDye Terminator Sequencing Kit V.2.1, Applied Biosystems]. We sequenced the *GPC5* coding sequence and flanking introns, the miR-17~92 cluster (chr13:92002859-92003645) (Primers are listed in Supplementary Table 2) and the putative miR-17a and miR-20a binding site in the 3' UTR of *MYCN* (chr2:16087062-16087085) in the 8 FS patients with no chromosomal rearrangements.

Supplementary Material

Refer to Web version on PubMed Central for supplementary material.

Acknowledgments

We are thankful to patients and their referent doctors for their active participation in this study. We are also particularly thankful to Dr Peter Hurlin, for generously providing forelimbs of *Mycn* cKO mouse embryos. This work was supported by grants from the Agence Nationale de la Recherche (ANR), the Fondation pour la Recherche Médicale (FRM), the INCa-DHOS, and the Institut National du Cancer. Work in the laboratory of A. V. was funded by NIH-NCI grant R01CA149707, a Sidney Kimmel Award, and a Geoffrey Beene Research Grant. E.Y. is a recipient of the NIH MCB T32 training grant. We thank Dr. Licia Selleri for her expertise in the phenotypic analysis of miR-17~92-mutant mice skeletons, Laurence Legeai-mallet, Anna Pelet and Paul Ogradowski for helpful discussion and technical advice, and Jennifer Hollenstein for editing the manuscript.

References

1. Mencia A, et al. Mutations in the seed region of human miR-96 are responsible for nonsyndromic progressive hearing loss. *Nat Genet.* 2009; 41:609–13. [PubMed: 19363479]
2. Fontana L, et al. Antagomir-17-5p abolishes the growth of therapy-resistant neuroblastoma through p21 and BIM. *PLoS ONE.* 2008; 3:e2236. [PubMed: 18493594]
3. Hayashita Y, et al. A polycistronic microRNA cluster, miR-17-92, is overexpressed in human lung cancers and enhances cell proliferation. *Cancer Res.* 2005; 65:9628–32. [PubMed: 16266980]
4. He L, et al. A microRNA polycistron as a potential human oncogene. *Nature.* 2005; 435:828–33. [PubMed: 15944707]

5. Mu P, et al. Genetic dissection of the miR-17~92 cluster of microRNAs in Myc-induced B-cell lymphomas. *Genes Dev.* 2009; 23:2806–11. [PubMed: 20008931]
6. Northcott PA, et al. The miR-17/92 polycistron is up-regulated in sonic hedgehog-driven medulloblastomas and induced by N-myc in sonic hedgehog-treated cerebellar neural precursors. *Cancer Res.* 2009; 69:3249–55. [PubMed: 19351822]
7. Olive V, et al. miR-19 is a key oncogenic component of mir-17-92. *Genes Dev.* 2009; 23:2839–49. [PubMed: 20008935]
8. Ota A, et al. Identification and characterization of a novel gene, C13orf25, as a target for 13q31-q32 amplification in malignant lymphoma. *Cancer Res.* 2004; 64:3087–95. [PubMed: 15126345]
9. Tagawa H, Seto M. A microRNA cluster as a target of genomic amplification in malignant lymphoma. *Leukemia.* 2005; 19:2013–6. [PubMed: 16167061]
10. Uziel T, et al. The miR-17~92 cluster collaborates with the Sonic Hedgehog pathway in medulloblastoma. *Proc Natl Acad Sci U S A.* 2009; 106:2812–7. [PubMed: 19196975]
11. Ventura A, et al. Targeted deletion reveals essential and overlapping functions of the miR-17 through 92 family of miRNA clusters. *Cell.* 2008; 132:875–86. [PubMed: 18329372]
12. Celli J, van Bokhoven H, Brunner HG. Feingold syndrome: clinical review and genetic mapping. *Am J Med Genet A.* 2003; 122A:294–300. [PubMed: 14518066]
13. Feingold M, Hall BD, Lacassie Y, Martinez-Frias ML. Syndrome of microcephaly, facial and hand abnormalities, tracheoesophageal fistula, duodenal atresia, and developmental delay. *American journal of medical genetics.* 1997; 69:245–9. [PubMed: 9096752]
14. van Bokhoven H, et al. MYCN haploinsufficiency is associated with reduced brain size and intestinal atresias in Feingold syndrome. *Nat Genet.* 2005; 37:465–7. [PubMed: 15821734]
15. Marcelis CL, et al. Genotype-phenotype correlations in MYCN-related Feingold syndrome. *Human mutation.* 2008; 29:1125–32. [PubMed: 18470948]
16. Firth HV, et al. DECIPHER: Database of Chromosomal Imbalance and Phenotype in Humans Using Ensembl Resources. *Am J Hum Genet.* 2009; 84:524–33. [PubMed: 19344873]
17. Morales JA, Mendizabal AP, Vasquez AI, Figuera LE, Gonzalez-Garcia JR. Interstitial deletion of 13q22-->q31: case report and review of the literature. *Clinical dysmorphism.* 2006; 15:139–43. [PubMed: 16760731]
18. Quelin C, et al. Twelve new patients with 13q deletion syndrome: genotype-phenotype analyses in progress. *European journal of medical genetics.* 2009; 52:41–6. [PubMed: 19022413]
19. Iafrate AJ, et al. Detection of large-scale variation in the human genome. *Nat Genet.* 2004; 36:949–51. [PubMed: 15286789]
20. Kidd JM, et al. Mapping and sequencing of structural variation from eight human genomes. *Nature.* 2008; 453:56–64. [PubMed: 18451855]
21. O'Donnell KA, Wentzel EA, Zeller KI, Dang CV, Mendell JT. c-Myc-regulated microRNAs modulate E2F1 expression. *Nature.* 2005; 435:839–43. [PubMed: 15944709]
22. Schulte JH, et al. MYCN regulates oncogenic MicroRNAs in neuroblastoma. *Int J Cancer.* 2008; 122:699–704. [PubMed: 17943719]
23. Stanton BR, Perkins AS, Tessarollo L, Sassoon DA, Parada LF. Loss of N-myc function results in embryonic lethality and failure of the epithelial component of the embryo to develop. *Genes & development.* 1992; 6:2235–47. [PubMed: 1459449]
24. Loven J, et al. MYCN-regulated microRNAs repress estrogen receptor-alpha (ESR1) expression and neuronal differentiation in human neuroblastoma. *Proceedings of the National Academy of Sciences of the United States of America.* 2010; 107:1553–8. [PubMed: 20080637]
25. Chen X, et al. Integration of external signaling pathways with the core transcriptional network in embryonic stem cells. *Cell.* 2008; 133:1106–17. [PubMed: 18555785]
26. Dews M, et al. Augmentation of tumor angiogenesis by a Myc-activated microRNA cluster. *Nat Genet.* 2006; 38:1060–5. [PubMed: 16878133]
27. Nagy A, et al. Dissecting the role of N-myc in development using a single targeting vector to generate a series of alleles. *Curr Biol.* 1998; 8:661–4. [PubMed: 9635194]

28. Moens CB, Auerbach AB, Conlon RA, Joyner AL, Rossant J. A targeted mutation reveals a role for N-myc in branching morphogenesis in the embryonic mouse lung. *Genes Dev.* 1992; 6:691–704. [PubMed: 1577267]
29. Ota S, Zhou ZQ, Keene DR, Knoepfler P, Hurlin PJ. Activities of N-Myc in the developing limb link control of skeletal size with digit separation. *Development.* 2007; 134:1583–92. [PubMed: 17360777]
30. Stanton BR, Perkins AS, Tessarollo L, Sassoon DA, Parada LF. Loss of N-myc function results in embryonic lethality and failure of the epithelial component of the embryo to develop. *Genes Dev.* 1992; 6:2235–47. [PubMed: 1459449]
31. Sawai S, et al. Defects of embryonic organogenesis resulting from targeted disruption of the N-myc gene in the mouse. *Development.* 1993; 117:1445–55. [PubMed: 8404543]
32. Mestdagh P, et al. The miR-17-92 microRNA cluster regulates multiple components of the TGF-beta pathway in neuroblastoma. *Mol Cell.* 2010; 40:762–73. [PubMed: 21145484]
33. Volinia S, et al. A microRNA expression signature of human solid tumors defines cancer gene targets. *Proc Natl Acad Sci U S A.* 2006; 103:2257–61. [PubMed: 16461460]
34. Dews M, et al. The myc-miR-17~92 axis blunts TGF{beta} signaling and production of multiple TGF{beta}-dependent antiangiogenic factors. *Cancer Res.* 2010; 70:8233–46. [PubMed: 20940405]
35. Cognet M, et al. Dissection of the MYCN locus in Feingold syndrome and isolated oesophageal atresia. *Eur J Hum Genet.* 2011
36. Masurel-Paulet A, et al. Delineation of 15q13.3 microdeletions. *Clin Genet.* 2010; 78:149–61. [PubMed: 20236110]

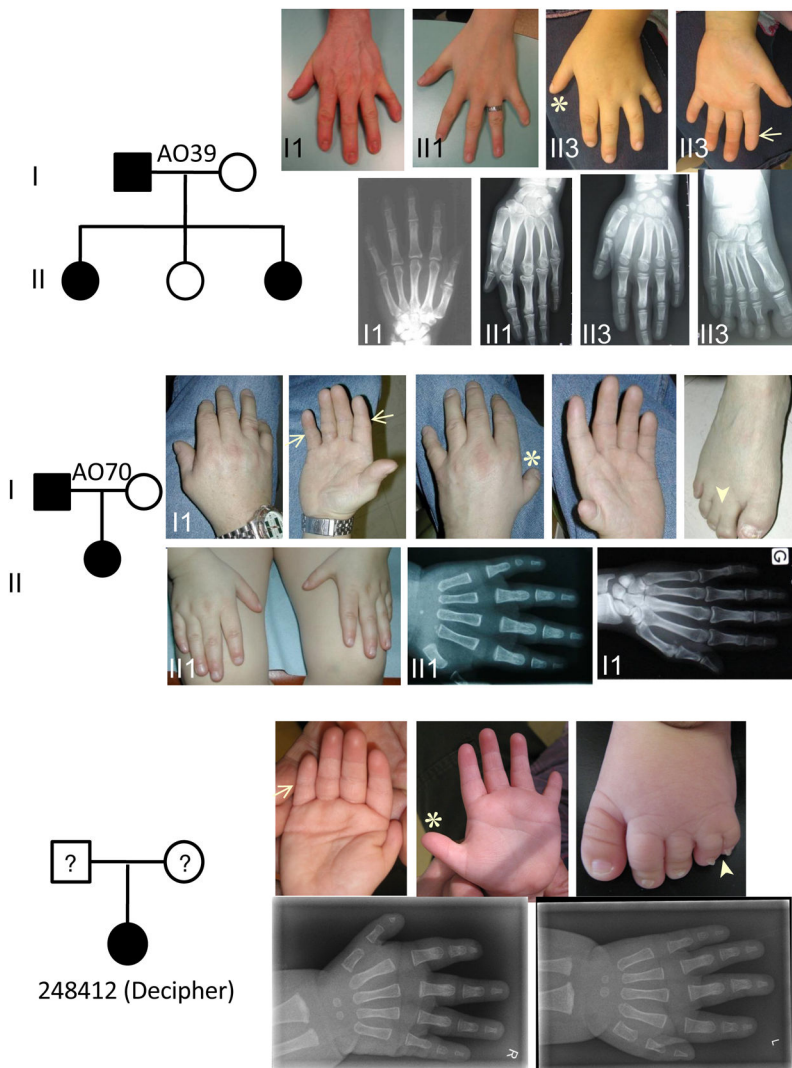
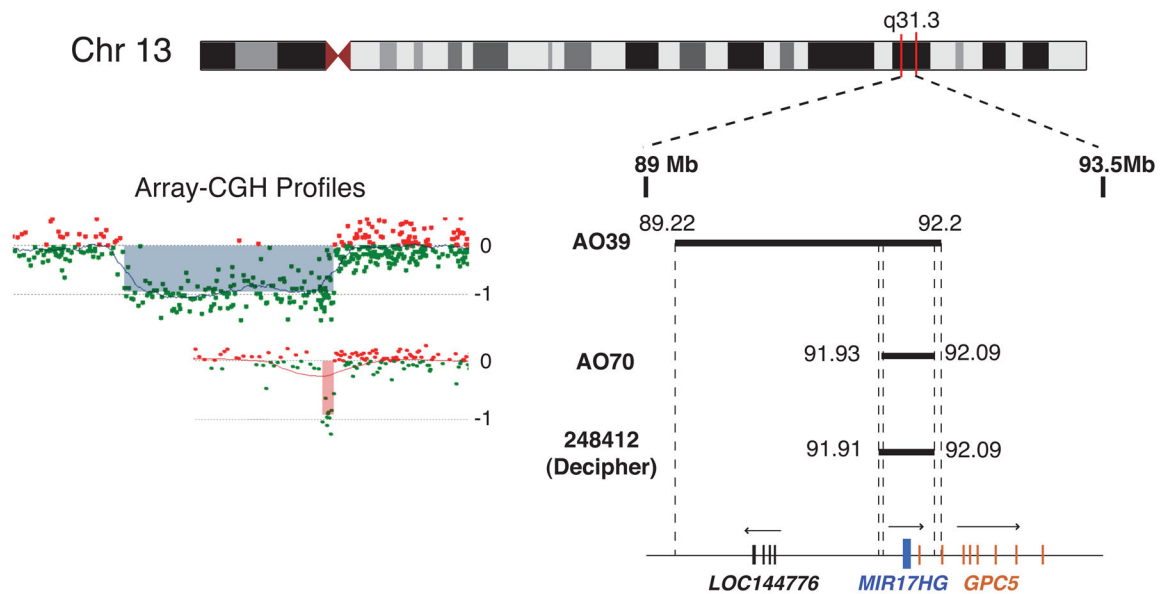


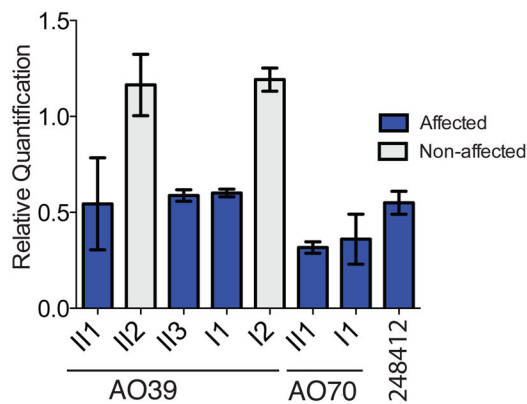
Figure 1. Clinical features of patients with del13q31.3

Clinical features and radiographs of affected individuals from families AO39, AO70 and patient 248412 showing brachydactyly, brachymesophalangy of the 2nd and 5th fingers (better appreciated on the palmar view, arrows), hypoplastic thumbs of variable severity (asterisks) and cutaneous syndactyly of toes (arrow heads).

A



B



C

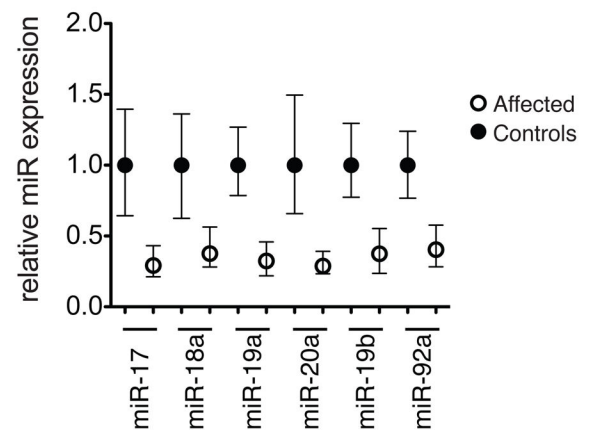


Figure 2. Mapping 13q31.3 microdeletions in FS patients

(a) Schematic illustration of the microdeletions identified in AO39 and AO70 families and Decipher patient 248412. (b) Genomic qPCR showing that the microdeletion segregates with the disease in families AO70 and AO39. (c) RT-qPCR showing reduced expression of individual microRNAs encoded by the miR-17~92 cluster in peripheral white blood cells of patients carrying 13q31.3 microdeletions (n=3) compared to healthy donors (n=4). For each miRNA, the mean relative expression and the range of expression (error bars) compared to control donors are shown.

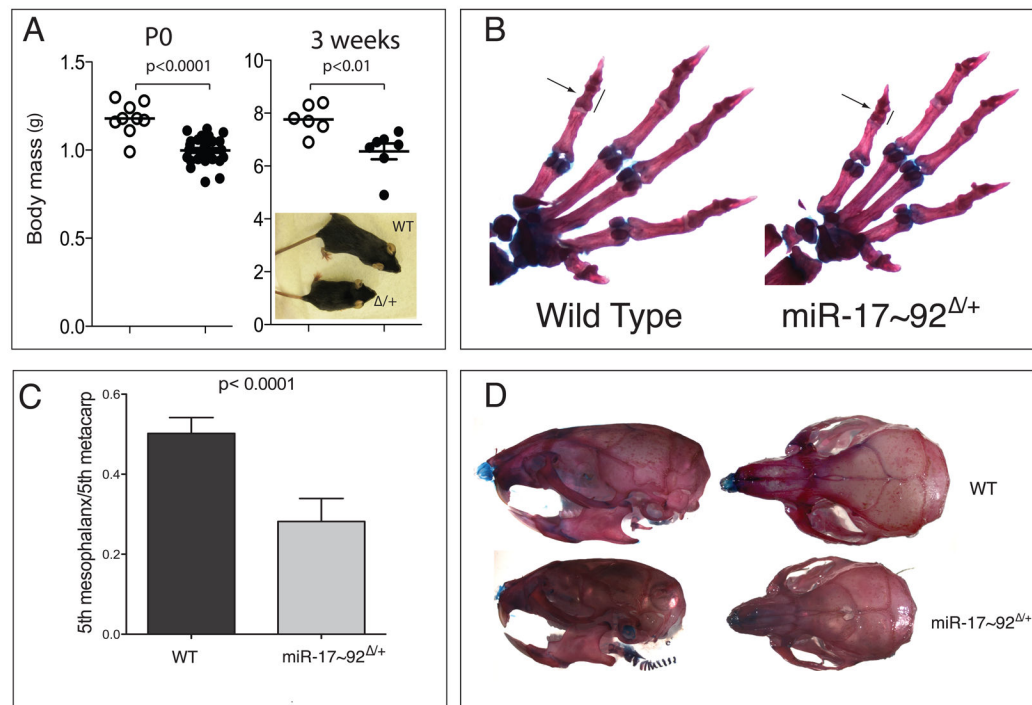


Figure 3. miR-17~92 ^{+/±} mice display features of FS

(a) Mice hemizygous for miR-17~92 are smaller than their wild-type littermates. Wild type (empty circles) and miR-17~92 ^{+/±} (filled circles) mice were weighed at P0 (left panel) or at weaning (3 weeks, right panel). P-value was computed using the two-tailed t-test. **(b)** Alcian blue and alizarin red staining of wild-type and miR-17~92 ^{+/±} forelimbs from female, age-matched mice. The 5th mesophalanx (arrow) is shorter in hemizygous animals compared to wild-type mice (bar). **(c)** Quantification of the relative length of the 5th mesophalanx in wild-type (n=6) and miR-17~92 ^{+/±} (n=10) murine forelimbs. The ratio between length of the 5th mesophalanx and length of the 5th metacarpal bone is plotted. Error bars = 1 standard deviation. **(d)** Lateral (left) and dorsal (right) views of mouse skulls of age-matched wild-type (top) and miR-17~92 ^{+/±} (bottom) male mice.

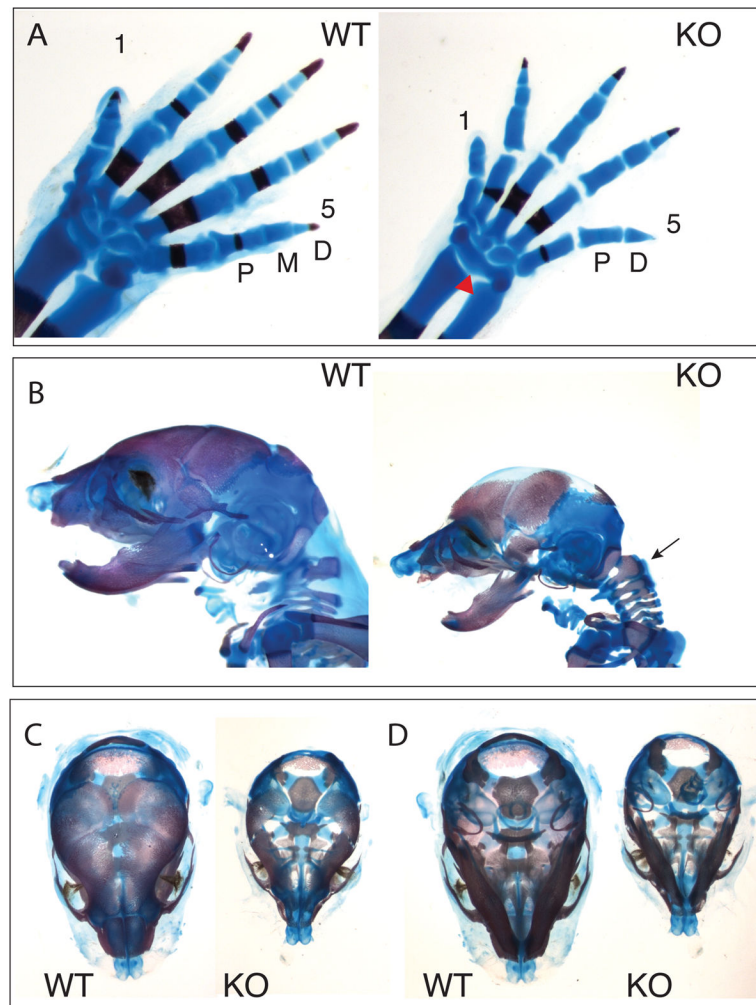


Figure 4. Widespread skeletal defects in E18.5 $miR-17\sim 92^{-/-}$ embryos

(a) Skeletal staining of the left hand of E18.5 littermate embryos. Notice the absence of the 5th mesophalanx (M) in the forelimb of the $miR-17\sim 92^{-/-}$ embryo (P= proximal, D = distal). Also notice the delayed ossification of metacarpal bones and of proximal phalanges, and the fusion of the first row of carpal bones (red arrowhead) in the mutant embryo. (b) Lateral views of embryonic skeletons showing delayed ossification of the skull and asymmetric fusions of the first three cervical vertebrae in the KO animals (arrow). (c) Dorsal and (d) ventral views of the skulls of $miR-17\sim 92^{-/-}$ and wild-type E18.5 embryos, showing microcephalia and delayed ossification of occipital, parietal and frontal bones in mutant embryos.